Xiao *et al. Energy Mater* 2021;1:100013
DOI: 10.20517/energymater.2021.17

Energy Materials

Review

Open Access

Check for updates

Recent advances in anion-derived SEIs for fast-charging and stable lithium batteries

Ye Xiao[1], Rui Xu[1], Lei Xu[1], Jun-Fan Ding[1], Jia-Qi Huang[2]

[1]School of Materials Science and Engineering, Beijing Institute of Technology, Beijing 100081, China.
[2]Advanced Research Institute of Multidisciplinary Science, Beijing Institute of Technology, Beijing 100081, China.

Correspondence to: Prof. Jia-Qi Huang, Advanced Research Institute of Multidisciplinary Science, Beijing Institute of Technology, 5 Zhongguancun South Street, Haidian District, Beijing 100081, China. E-mail: jqhuang@bit.edu.cn

How to cite this article: Xiao Y, Xu R, Xu L, Ding JF, Huang JQ. Recent advances in anion-derived SEIs for fast-charging and stable lithium batteries. *Energy Mater* 2021;1:100013. https://dx.doi.org/10.20517/energymater.2021.17

Received: 1 Oct 2021 **First Decision:** 20 Oct 2021 **Revised:** 27 Oct 2021 **Accepted:** 5 Nov 2021 **Published:** 22 Nov 2021

Academic Editor: Yuping Wu **Copy Editor:** Yue-Yue Zhang **Production Editor:** Yue-Yue Zhang

Abstract

The construction of stable and reliable electrode interfaces is one of the key scientific issues widely encountered by the battery community. An anion-derived solid electrolyte interphase (SEI) has been recently reported to outperform the traditional solvent-rich SEI in inhibiting side reactions, motivating ion transport and regulating electrode reactions in working Li batteries. Here, we first explicitly introduce the fundamental characteristics of anion-derived SEIs and then concisely present novel developments in electrolyte chemistry involving highly concentrated, localized highly concentrated and weakly solvating electrolytes, which facilitate the formation of anion-derived SEIs on anodes. The critical significance of these SEIs for building fast-charging and stable Li batteries is particularly highlighted. Finally, we outline the future challenges of designing Li metal interfaces to further enhance the cycling reversibility and lifespan of working batteries.

Keywords: Lithium metal anode, solid electrolyte interphases, highly concentrated electrolytes, weakly solvating electrolytes, anion-derived SEIs

INTRODUCTION

Human activities have resulted in significant climate change[1]. Global warming and frequent extreme weather events, such as high temperatures and heavy rainfall, have highlighted the urgent need for sustainable development[2,3]. Sustainability has become a top priority in modern society and is highly

associated with the exploitation and further storage of renewable energy[4-6]. Advanced energy storage devices, particularly lithium-ion batteries (LIBs) facilitate the high-efficiency storage and conversion of renewable energy[7] and also boost electrification by promoting the booming development of electric vehicles and novel electronic devices[8,9]. To further unlock the upper limit of conventional LIBs with regards to energy density, the Li metal anode has recently been revived for building next-generation high-energy-density batteries (> 350 Wh kg^{-1})[10-12]. However, the practical deployment of Li metal batteries is significantly hampered by their short lifespan and poor safety[13], which are inherently triggered by the unstable solid electrolyte interphases (SEIs) formed on Li anodes[14,15].

As the locations where electrode reactions occur, electrode interfaces play an important role in dominating battery performance[16-18]. Given the generally low working potential of anodes, electrolyte components, including the solvent and anion, become readily reduced to constitute the solid products at the interface, i.e., the SEI[19]. A native SEI is featured with chemical and structural heterogeneity due to a variety of intricate factors[20]. From the perspective of thermodynamics, the highest occupied molecular orbital and lowest unoccupied molecular orbital (LUMO) of the electrolyte components determine the ease of their decomposition against oxidation and reduction, respectively[21]. Dynamically, the adsorption behavior of electrolyte components at the electrode interfaces predominates the formation of the initial SEI[22], while the solvation behavior of the electrolyte further affects its subsequent evolution[19]. These factors are closely linked with each other. For example, the complexation with electron-withdrawing Li^+ reduces the LUMO energy of electrolyte components, making it thermodynamically easier to be reduced by anodes[23]. Furthermore, the varying electrode potential changes the electrical properties of the electrodes, thereby further thermodynamically or kinetically affecting the above aspects[24-26]. On this basis, the complex reduction pathways of the multiple components in the electrolyte generate random SEIs with intrinsic heterogeneity[27,28]. More adversely, the huge volume deformation of the electrode during cycling further introduces stress effects and aggravates interfacial instability[29]. Such an unstable SEI will undergo continuous cracking and reconstruction, which not only consumes the active capacity but also gradually thickens, resulting in an increase in cell polarization[30].

With regards to the above dilemma, extensive research has been focused on the regulation of electrode interfaces in terms of composition[31-34], structure[35-37] and mechanical properties[38-40] by designing a robust, uniform and kinetically favorable SEI[41,42], thereby paving the way for the construction of stable and fast-charging Li batteries. Recently, anion-derived SEIs have attracted significant research interest and have been considered as ideal SEIs for enhancing the cycling reversibility of graphite and Li electrodes[43]. By rationally adjusting the solvation structure of Li^+, the decomposition of anions can be promoted and the conventional interfacial chemistry dominated by solvents can be thus modified[44]. The as-obtained SEI with multiple desired characteristics provides feasible outlets to overcome the current dilemma encountered by working Li metal anodes, such as low Coulombic efficiency (CE), short lifespan and poor safety [Figure 1][45].

Herein, the critical characteristics of anion-derived SEIs are first presented to provide a comprehensive landscape. Second, this review summarizes the key progress and basic understanding in constructing anion-derived SEIs via regulating the solvation structure of the electrolyte. Three typical types of electrolyte chemistry, namely, highly concentrated electrolytes (HCEs), localized highly concentrated electrolytes (LHCEs) and weakly solvating electrolytes (WSEs), for facilitating anion-derived SEI formation are specifically introduced. Finally, future research challenges in designing stable Li metal interfaces are discussed.

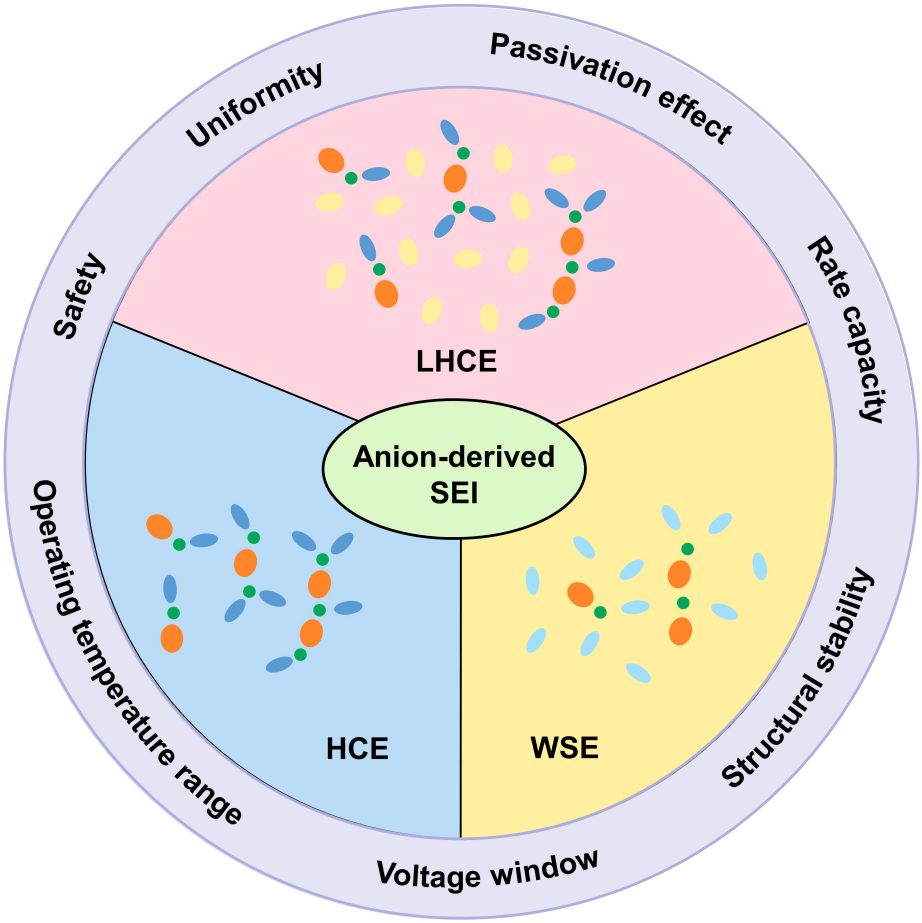

Figure 1. Schematic diagram of the design strategy for anion-derived SEIs by solvation structure regulation. SEI: Solid electrolyte interphase; LHCE: localized highly concentrated electrolyte; HCE: highly concentrated electrolyte; WSE: weakly solvating electrolyte.

CHARACTERISTICS OF ANION-DERIVED SEIS

The characteristics of anion-derived SEIs determine the function of electrode/electrolyte interfaces, which in turn affects the overall performance of batteries. The relevant characteristics of anion-derived SEIs are presented from the perspectives of nucleation pattern, chemistry and structure and kinetic properties, thereby providing general insights for understanding interfacial effects.

Nucleation and growth

Different from the formation scenario of solvent-derived SEIs, the nucleation and early growth of anion-derived SEIs on graphite anodes can be well described with a surface reaction-controlled two-dimensional progressive nucleation and growth model[46-49]. Such a unique nucleation feature can be captured from the voltage pit detected during galvanostatic operation exclusively in electrolytes favoring anion decomposition. This behavior is similar to the nucleation process of Li in Li||Cu cells and Li_2S in Li-S cells[50], which has been explained from the perspective of the poor solubility and weak affinity of the anion decomposition products with the electrolyte. The chemistry and structure of atomically distributed anion-derived SEIs can be clearly verified via atomic force microscopy [Figure 2A][46].

Chemistry and structure

Generally, anions with a larger radius, such as hexafluorophosphate (PF_6^-), difluoro(oxalato)borate ($DFOB^-$),

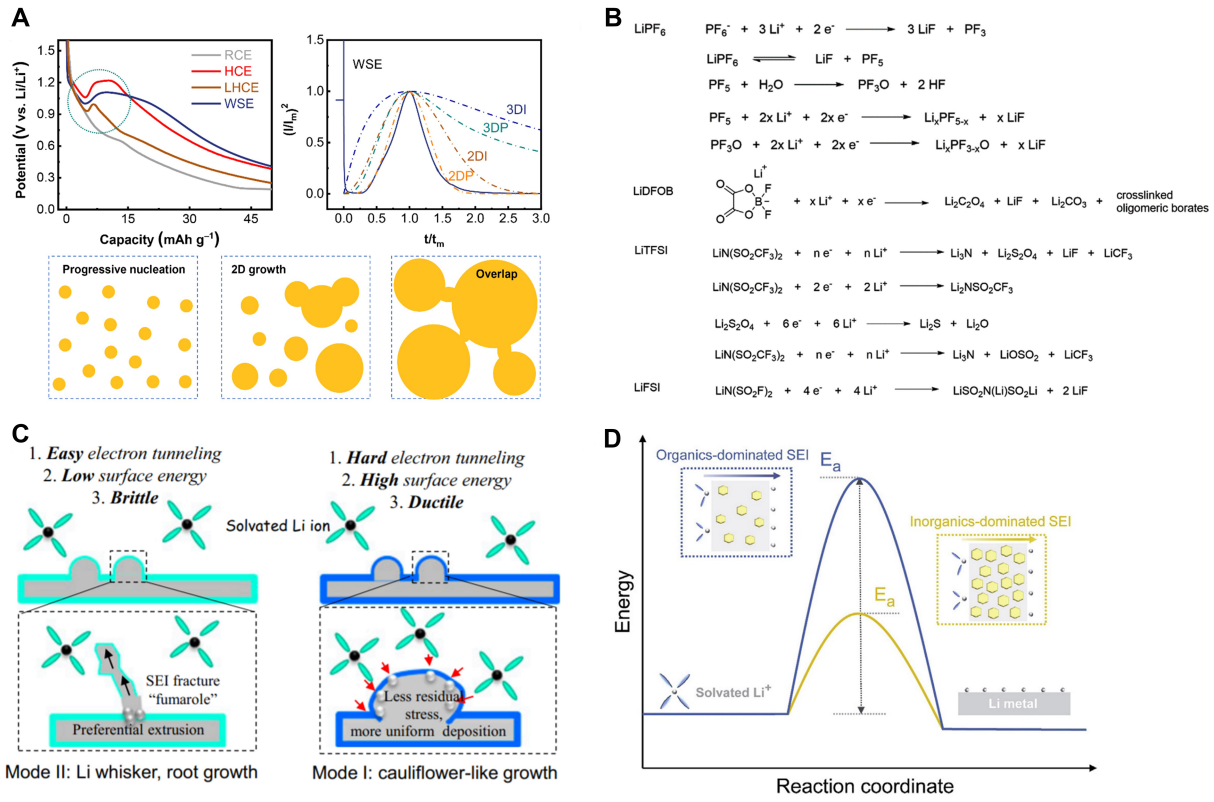

Figure 2. Characteristics of anion-derived solid electrolyte interphases (SEIs). (A) Abnormal voltage pit and comparison and schematic diagram of the two-dimensional (2D) progressive nucleation and growth of anion-derived SEIs. Reproduced with permission[46] (copyright 2021, Wiley VCH GmbH). (B) Reductive decomposition products of various lithium salts in the process of forming an SEI. Reproduced with permission[51] (copyright 2020, Wiley VCH GmbH). (C) Lithium growth modes under the influence of different interfaces. Adapted with permission[52] [copyright 2018, the author(s)]. (D) Reduced activation energy (E_a) for Li^+ desolvation and diffusion across an SEI. Reproduced with permission[53] (copyright 2019, Elsevier).

bis(fluorosulfonyl)imide (FSI^-) and bis(trifluoromethane)sulfonimide ($TFSI^-$), with negative charges that are more dispersed and thus prone to dissociation with Li^+, are selected in order to ensure reasonable solubility of the lithium salt in non-aqueous solvents[54]. The decomposition products of the anions are almost inorganic substances, as shown in Figure 2B[51].

Lithium fluoride (LiF), lithium nitride (Li_3N), lithium sulfide (Li_2S), lithium oxide (Li_2O) and so on are typical constituents in anion-derived SEIs, which are present in a mosaic structure with polycrystalline domains[55]. Compared with the organic oligomers mainly resulting from solvent reduction, these inorganic components generally feature larger bandgaps, higher mechanical stiffness and lower reduction reactivity [Figure 2C][52]. For example, LiF has a wide bandgap of 8.9 eV and a Young's modulus of 55 GPa[56,57]. Numerous methods for constructing LiF-rich SEIs have been employed to stabilize the interface, including gas phase reactions[58] and the use of additives[31] and artificial interfaces[35], which can simultaneously inhibit continuous electrolyte decomposition and the growth of dendrites[59]. Li_3N with a high ionic conductivity ($\sim 10^{-3}$ S cm^{-1}) is also regarded as a favorable SEI component to passivate the interface and accelerate the interfacial dynamics[60,61]. With a bandgap of 4.7 eV and a Young's modulus of 108 GPa[57,62], Li_2O has an excellent ability to suppress electron tunneling and stability against Li, resulting from the low oxidation state[63].

A variety of inorganic components can complement each other and bestow excellent properties to inorganic-rich SEIs[64]. These properties synergistically equip the anion-derived SEIs with enhanced electron insulation at a relatively thin thickness, modulus and uniformity to mechanically resist dendrite penetration, as well as improved chemical compatibility against Li metal to improve the interfacial stability. Furthermore, the robust and uniform SEI structure is highly beneficial to the homogeneous release of stress so that the interfacial integrity can be better maintained. As described by Shen *et al.*[65], a moderate elastic modulus of 3.0 GPa with high structural uniformity can enhance the mechanical stability of SEIs.

Kinetic properties

Anion-derived SEIs with inorganic-rich polycrystalline domains have abundant grain boundaries. Compared with bulk lattice conduction, the energy barrier of Li diffusion through grain boundaries was calculated to be lower and the migration rate is faster[66,67]. The interfaces between different inorganic phases also represent imperative routes for ion transport. Based on the systematic analysis of interfacial kinetics in model systems, inorganic-rich anion-derived SEIs were discovered to decrease the activation energy for both Li^+ desolvation and diffusion [Figure 2D][53]. Aside from the intrinsic kinetic characteristics, the reduced thickness at the whole SEI scale also contributes to expedited kinetics for the interfacial ion transport step. The fast interfacial transport kinetics increase the available concentration of Li^+ beneath the SEI and the Li deposition turns into a reaction-controlled process, which was deduced as the origin of the spherical Li deposition morphology[68]. In addition, inorganics have a higher surface energy than organics, which facilitates lateral diffusion while restricting vertical dendrite growth[52,69]. The related parameters of different SEI components are presented in Table 1. Collectively, these favorable properties of anion-derived SEIs fundamentally promise the fast-charging function and high stability of working batteries.

SOLVATION REGULATION IN ANION-DERIVED SEIS

Despite the attractive features of anion-derived SEIs, SEI formation in conventional dilute non-aqueous electrolytes is predominately controlled by solvent decomposition. This is ascribed to the preferential solvation of strong electron-donating solvents around Li^+ in these electrolytes. Generally, solvation involves complex electrostatic interactions among cations, anions and solvent molecules. The competitive coordination of anions and solvents with Li^+ determines the solubility of lithium salts, as well as the structure of the solvation clusters [Figure 3A][76].

The salt concentration is a critical factor in determining the Li^+ solvation structure. In traditional dilute solutions, the dipole-ion interaction between the solvent molecules and Li^+ separates the cations from anions to form solvent-separated ion pairs, which govern the Li^+ solvation environment[77]. As the salt concentration increases, less free solvent is available to occupy the solvation sheath, thereby allowing anions to interplay with Li^+[78]. Solvated clusters containing anions such as contact ion pairs (CIPs) and aggregates (AGGs) appear, in which the anion is coordinated with one, two or more cations[79]. Furthermore, once the intrinsic solvating power of the solvents towards Li^+ is rationally designed, anions can also largely participate in the Li^+ solvation shell, although the salt concentration is maintained at a relatively low level [Figure 3B][80]. The aggregation of anion in the solvation structure of Li^+ builds the basis for the anion-derived SEI formation. These strategies regarding solvation regulation in HCEs, LHCEs and WSEs are specifically introduced in this section. The basic physicochemical properties of these electrolytes are compared in Table 2.

HCEs

The common concentration of aprotic electrolytes is ~1.0 M given the tradeoff between conductivity, solubility and viscosity[77]. When the solution concentration exceeds 3.0 M, although the viscosity and ionic

Table 1. Comparison of bulk ($E_{m,b}$) and surface ($E_{m,s}$) Li^+ migration energy barriers and calculated interfacial energies of different compounds

Compound	$E_{m,b}$ (eV)	$E_{m,s}$ (eV)	γ (meV Å^{-2})
LiF	0.729[57]	0.19[70]	73.28[71]
Li_3N	0.007-0.038[72]	-	77.5[73]
Li_2S	0.270[74]	-	19.01[71]
Li_2O	0.152[57]	0.31[70]	38.70[71]
Li_2EDC	0.640[75]	-	-

Table 2. Physicochemical properties of conventional electrolyte, HCE, LHCE and WSE

Electrolyte	Conductivity (mS cm^{-1})	Viscosity (cP)	Mole ratio (solvent/salt)	Transference number (Li^+)	Density (g cm^{-3})
Conventional electrolyte	> 10[78]	< 5[81,82]	> 5[83]	< 0.4[84]	< 1.2[83]
HCE	< 10[85-87]	> 10[88-90]	< 5[75,85,91]	> 0.5[81]	> 1.2[88,91]
LHCE	1-10[92-94]	5-10[94-96]	> 3[97,98]	> 0.5[99]	> 1.2[98]
WSE	2-10[80]	< 5[100,101]	> 5[102]	> 0.5[101]	~1[100]

LHCE: Localized highly concentrated electrolyte; HCE: highly concentrated electrolyte; WSE: weakly solvating electrolyte.

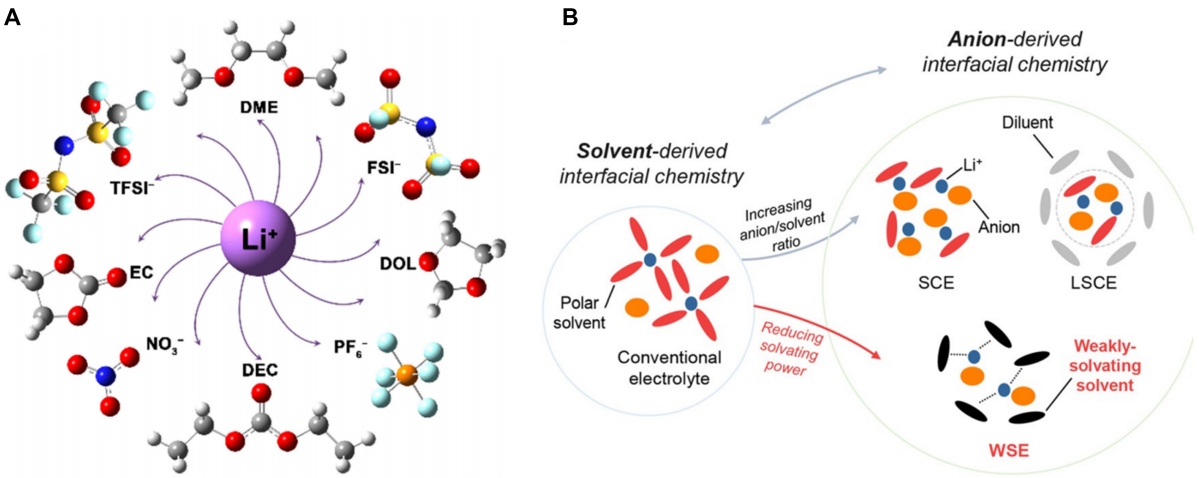

Figure 3. Solvation interaction and structure. (A) Interaction between solvents and anions with Li^+. Reproduced with permission[76] (copyright 2019, Wiley VCH Verlag GmbH & Co. KGaA, Weinheim). (B) Solvation structures in conventional electrolyte, HCE, LHCE and WSE. Reproduced with permission[80] (copyright 2019, Wiley VCH GmbH). LHCE: Localized highly concentrated electrolyte; HCE: highly concentrated electrolyte; WSE: weakly solvating electrolyte; DME: dimethoxyethane; FSI^-: bis(fluorosulfonyl)imide; PF_6^-: hexafluorophosphate; DEC: diethyl carbonate; $TFSI^-$: bis(trifluoromethane)sulfonimide.

conductivity of the electrolyte are sacrificed to some extent, the altered solvation structure and the resulting interfacial chemistry bring a series of unexpected functionalities[78].

HCEs were initially discovered to inhibit the co-intercalation of propylene carbonate (PC) in graphite due to the optimized interfacial properties [Figure 4A][103], which expanded the choice of electrolyte systems beyond ethylene carbonate[104]. This is of paramount significance, especially for the exploitation of low-temperature and fast-charging LIBs. By combining experiments and theoretical calculations, Yamada *et al.*[90] revealed the correlation between the unique solvation structure in HCEs and the interfacial chemistry formed at the electrode surface. Using Raman spectroscopy and X-ray photoelectron

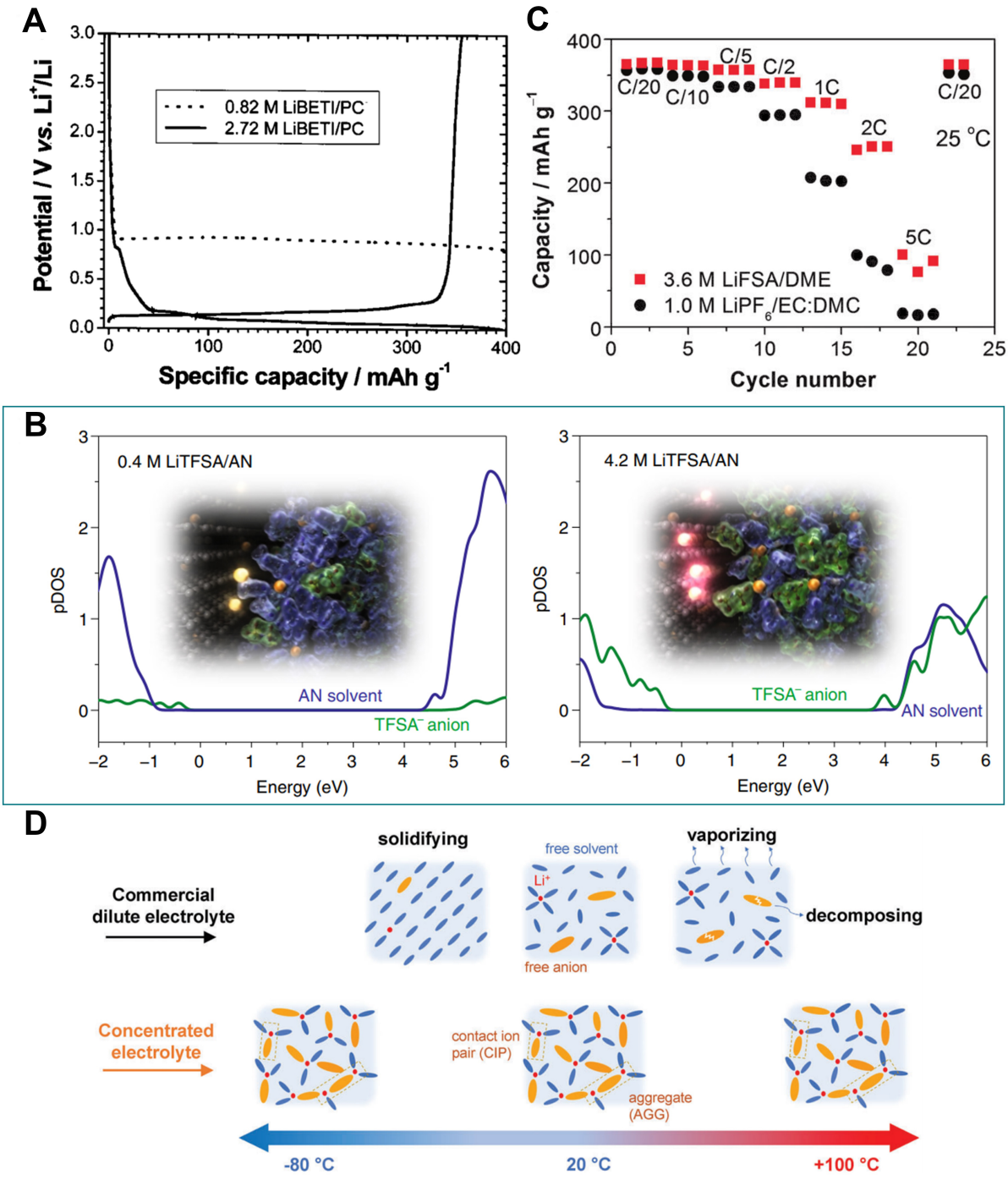

Figure 4. Performance comparison of HCEs and dilute electrolytes. (A) Initial charge/discharge curves of natural graphite in electrolytes with different concentrations. Reproduced with permission[103] (copyright 2002, IOP Publishing). (B) Projected density of states of dilute and concentrated LiTFSA/AN electrolytes. Insets display the interface between the graphite electrode and electrolyte. Reproduced with permission[45] (copyright 2019, Springer Nature Limited). (C) Rate performance of natural graphite||Li cells using a highly concentrated electrolyte (HCE) and commercial electrolyte. Reproduced with permission[106] (copyright 2013, Royal Society of Chemistry). (D) Solvation structures in dilute electrolyte and HCE from -80 to 100 °C. Adapted with permission[107] [copyright 2021, the author(s)].

spectroscopy (XPS), the bulk structure of a 4.2 M LiTFSI/acetonitrile (AN) HCE, with few free solvent molecules and more coordinated anions, and the anion-dominated interfacial chemistry were clearly

identified, respectively. Density functional theory (DFT)-based molecular dynamics revealed a correlation where anions supplied electrons to Li^+ due to the enhanced interaction between them, resulting in a decrease in their own orbital level. This transfers the LUMO energy from the AN solvent to the $TFSI^-$ anion at high concentrations [Figure 4B][45]. Accordingly, the lithium salt anion was preferentially reduced to form an anion-derived SEI, which further prevented the decomposition of vulnerable AN and enhanced the electrochemical performance of the HCE.

Furthermore, an increase in the equilibrium potential of electrode reactions caused by the higher Li^+ activity in HCEs also contributes to the mitigation of solvent reduction[105]. The anion-derived interfacial chemistry intensively enhanced the rate capacity at up to 5 C, highlighting the crucial role of interfacial kinetics compared to the bulk transport properties. An enhanced rate performance compared to a commercial carbonate electrolyte was also demonstrated in LIBs using a 3.6 M LiFSI/1,2-dimethoxyethane (DME) HCE, despite the reduced ionic conductivity and increased viscosity of the bulk electrolyte [Figure 4C][106]. Wang *et al.*[107] reported a 4.0 M LiFSI/dimethyl carbonate (DMC) electrolyte that could afford better rate performance at low temperatures and normal operation at high temperatures [Figure 4D]. The establishment of a stable Li^+-conductive interface compensated for the inferior bulk conductivity, while the thermal stability of the HCE itself combined with the robust anion-derived interface prevented battery failure resulting from gas evolution and the collapse of cathode structures.

Therefore, an interfacial transport rate-determining step can be recognized. The interfacial transport journey of a solvated Li^+ involves desolvation, interfacial mass transfer and charge transfer processes[43]. HCEs boost the interfacial kinetics from three possible aspects: (1) a high pre-exponential factor due to the high interfacial Li^+ concentration; (2) a kinetically favorable SEI for fast ion transport; and (3) a distinct desolvation behavior of Li^+ from CIP and AGG structures compared to that from solvent-separated ion pairs. However, the bulk ionic conductivity of the electrolyte becomes a critical factor for the fast charging of energy-type cells where thick porous electrodes are employed[43].

Similar to the protective SEI generated by EC[108], an anion-derived SEI is sufficiently dense and compact to effectively suppress the co-intercalation and decomposition of solvents, guaranteeing the high reversibility of Li^+ intercalation/deintercalation in graphite[109]. By simply increasing the salt concentration, Wang *et al.*[87] demonstrated that the incompatibility between flame-retardant trimethyl phosphate and a carbon anode could be largely overcome [Figure 5A]. This resulted from the spontaneous formation of a robust inorganic passivation film on the anode. In addition, such a dynamic stability may come from the alleviated dissolution of SEI components in HCEs with a reduced solvent activity[81], as some researches have reported that the anion-derived SEIs formed in HCEs cannot function well in the corresponding dilute solution[110]. Ming *et al.*[111] proposed that the solvation structure also contributed to the stable cycling of graphite electrodes other than the effect of the SEI, because they found that the as-formed SEI could not prevent the solvent co-intercalation once the film-forming additive was removed. The introduction of additives weakened the Li^+-solvent interaction and promoted a facile desolvation process, thereby inhibiting the co-intercalation of solvents. The intercalation of naked Li^+ is subjected to the desolvation step[112]. From the perspective of free solvent activity, Moon *et al.*[110] elucidated that Li^+ intercalation had a higher electrode potential than co-intercalation in concentrated electrolytes with a low solvent activity, so that solvent co-intercalation in concentrated electrolytes could be avoided.

The application of HCEs has also been validated as a feasible strategy to pronouncedly improve the reversibility of fast-rate Li metal anodes[113]. Using a 4.0 M LiFSI/DME electrolyte, Qian *et al.*[85] reported the stable and high-efficiency cycling of Li||Cu cells, which showed a steady CE of 98.4% at 4.0 mA cm^{-2} for over

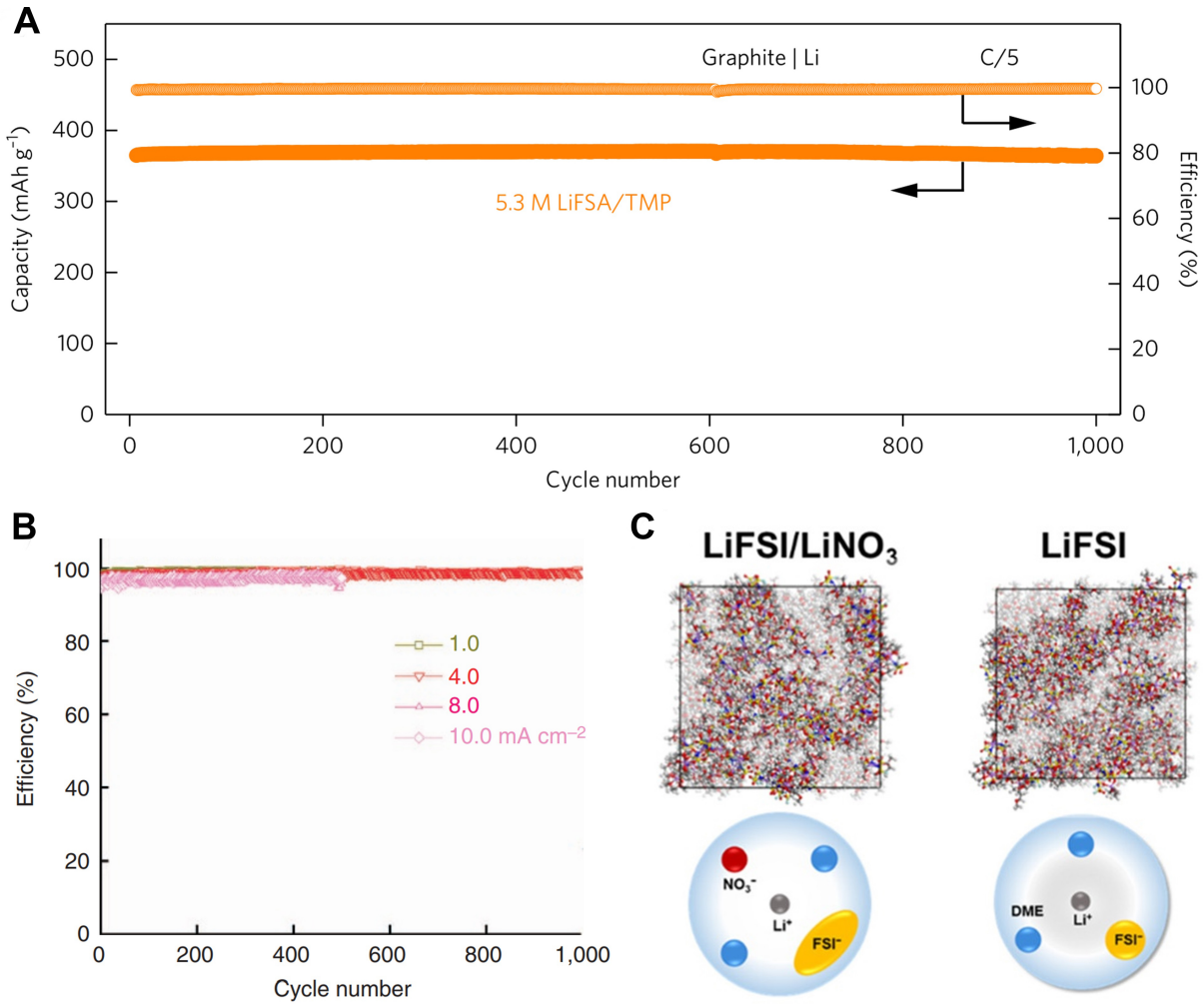

Figure 5. Electrochemical performance and characteristics of HCEs. (A) Cycling performance of graphite||Li half cell using a HCE. Adapted with permission[87] [copyright 2017, the author(s)]. (B) CE of Li||Cu half cells in 4.0 M LiFSI/DME at various current densities. Adapted with permission[85] [copyright 2015, the author(s)]. (C) Molecular dynamics snapshots of 0.2 M $LiNO_3$+2.0 M LiFSI/DME and 2.2 M LiFSI/DME electrolytes (top). Colors correspond to different atoms and solvent states: H-white; Li-purple; C-gray; O-red; N-blue; F-green; S-yellow; unsolvated solvents-gray. Schematics of Li^+ solvation structures (bottom). Reproduced with permission[115] (copyright 2019, American Chemical Society).

1000 cycles and 97% even at 10.0 mA cm^{-2} for over 500 cycles [Figure 5B]. Such superior Li performance at high rates can be explained from the flat Li deposition behavior under the thin, uniform and conductive SEI. In such a high concentration regime, the anion constitutions can also be designed to intentionally regulate the SEI chemistry. Utilizing ab initio molecular dynamics simulations, Alvarado *et al.*[114] revealed the important role of the competitive decomposition kinetics between FSI^- and $TFSI^-$ anions in the bis-salt system, i.e., the mutual modulation effect promoted the generation of a uniform and inorganic SEI.

Zhang *et al.*[115] found that the introduction of 0.2 M $LiNO_3$ in 2.0 M LiFSI/DME not only contributed to the construction of a SEI by its own reduction, but also modulated the coordination mode between the primal anions and Li^+, thereby promoting the complete decomposition of polarized FSI^- [Figure 5C]. The generated LiF, Li_2SO_x and LiN_xO_y synergistically homogenized SEI and Li deposition, thereby elevating the cycling reversibility of Li metal anodes. In another work, a dual-salt electrolyte of 2.0 M LiDFOB+1.4 M $LiBF_4$ /FEC:DEC (v:v = 1:2) promoted synergistically tightly packed Li deposition behavior, which not only

extended the cycling life of anode-free cells, but also significantly improved the battery safety[116]. In addition to stabilizing the anode interfaces, functional double-salt electrolytes are also beneficial for the stable operation of cathodes. Using 2.0 M LiTFSI+2.0 M LiDFOB/DME, Jiao *et al.*[88] realized the effective passivation of Li electrodes and high-voltage $LiNi_{1/3}Mn_{1/3}Co_{1/3}O_2$ (NCM) cathodes via the formation of thin and B-induced polymeric interfaces. This provided a promising method to enable ether-based electrolytes with superior reductive stability for applications in high-voltage Li metal batteries.

Furthermore, HCEs possess other merits in batteries besides promoting the anion-derived SEI formation, such as widening the oxidation window[86] and operation temperature of the cell, resisting the corrosion of the current collector[83] and alleviating the dissolution of transient metal ions from high-voltage cathodes[82]. As these aspects are beyond the scope of this review, they are not specifically discussed herein.

LHCEs

HCEs exert compelling performance at the expense of viscosity and cost, which is fatal to their practical application[45]. The viscosity of electrolytes affects the wetting to the separators and electrodes. HCEs with ten times or higher viscosity render a significantly prolonged formation time, especially for the use of thick electrodes[97]. Lithium salts represent the main cost of traditional electrolytes due to their high price and the cost increase brought by HCEs with a higher proportion of lithium salts makes them unacceptable for commercial applications. The employment of LHCEs considerably tackles this dilemma. LHCEs are obtained by diluting HCEs with a low-polarity inert solvent that is miscible with them. Low-viscosity hydrofluoroethers (HFEs) are often chosen as the diluent, where the -F groups close to the ether bond can reduce the electron cloud density of oxygen atoms, thereby weakening the ion-dipole interaction[117]. On this basis, LHCEs still retain the solvation structure of HCEs, while the overall concentration and viscosity of the electrolyte can be largely decreased. Hence, the anion-derived interfacial properties are preserved to a large extent. Consequently, LHCEs have become promising electrolyte systems for practical applications and attract tremendous research interest[92,96,118].

The initial prototype LHCE was first applied to Li-S batteries[119]. For the pursuit of high-rate capability, Dokko *et al.*[119] screened out a HFE solvent for a HCE of [Li(tetraglyme)$_1$][TFSI], 1,1,2,2-tetrafluoroethyl-2,2,3,3-tetrafluoropropyl ether (TTE), according to the criteria of high chemical stability, low polarity and miscibility. The introduction of TTE lowers the electrolyte viscosity and expedites mass transfer, while retaining the solvation structure of the HCE and its functions [Figure 6A].

A similar electrolyte system was also implemented in LIBs, as manifested in Figure 6B[120]. Solvent activity, the concentration of free solvents, is considered as a critical factor in determining the oxidative stability of electrolytes, the corrosion of aluminum current collectors, the intercalation or co-intercalation and the solubility of intermediates. In 2018, Chen *et al.*[98] explicitly proposed the concept of LHCEs. Two thirds of DMC solvent by molarity were replaced by a bis(2,2,2-tri-fluoroethyl) ether diluent in the original 5.5 M LiFSI/DMC electrolyte. A high-voltage Li metal battery using such a LHCE realized stable cycling exceeding the HCE counterpart and the anion-derived SEI that was rich in LiF and Li_2O dedicated to the dendrite-free deposition morphology. Chen *et al.*[98] successively published several articles on the applications of LHCEs in Li metal batteries by incorporating functional base solvents and diluents. Benefitting from the increased wettability and conduction properties compared to HCEs, Li||NCM batteries using a sulfone-based LHCE exhibited better rate and low-temperature performance [Figure 6C][94]. With the addition of the inert TTE diluent, the LUMO energy level further shifted to LiFSI, which mitigated the side reaction between solvents and the Li anode and facilitated the complete decomposition of anions to form a SEI with nitrogen-rich species [Figure 6D][94], resulting in uniform and rapid Li deposition behavior.

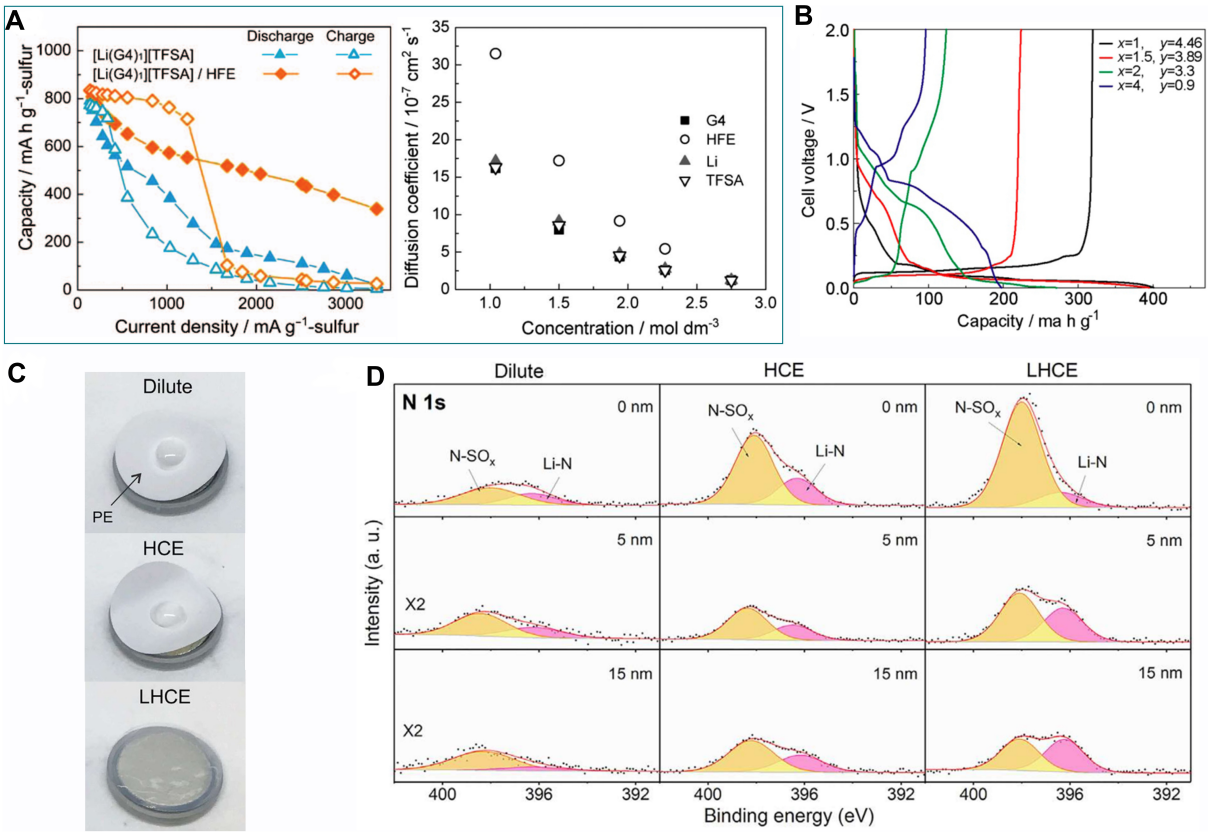

Figure 6. Characteristics and electrochemical performance of LHCEs. (A) Rate performance of Li-S batteries using HCE and LHCE, and the self-diffusion coefficients of each component in the LHCE. Reproduced with permission[119] (copyright 2013, IOP Publishing). (B) Charge/discharge curve of graphite||Li cells under different solvent/diluent ratios (1 M LiTFSI-*x*G3-*y*HFE). Reproduced with permission[120] (copyright 2015, American Chemical Society). (C) Wettability of dilute electrolyte, HCE and LHCE towards polyethylene separators. (D) N 1s spectra of SEI in three electrolytes at different sputtering depths. Reproduced with permission[94] (copyright 2018, Elsevier). LHCE: Localized highly concentrated electrolyte; HCE: highly concentrated electrolyte; HFE: hydrofluoroether.

Figure 7A demonstrated the densest deposition morphology in a LHCE composed of plated lithium chunks[121]. In another work, the SEI structure on the surface of Li anodes in the LHCE was clearly distinguished with the help of atomic-view cryo-electron microscopy, as revealed in Figure 7B[122]. A monolithic SEI with a thickness of 10 nm uniformly covered the surface of metallic Li, consisting of inorganics derived from anions. The amorphous structure of the anion-derived SEI may be the reason for the highly reversible Li plating/stripping. The LHCE effectively regulates dense and uniform Li deposition, as described above. Based on this, Cai *et al.*[123] determined that the LHCE increases the safe lithium-plating boundary in LIBs to 25% of the lithiation capacity. The plated Li was evenly distributed on the surface of graphite particles and there was scarcely any "dead lithium" signal at the delithiated state according to time-of-flight secondary ion mass spectrometry results, as depicted in Figure 7C[123]. Recently, Jiang *et al.*[89] probed the fast-charging performance of graphite half cells using a 1.5 M LiFSI/DME:bis(2,2,2-trifluoroethyl) ether (v:v = 1:2) electrolyte. Benefitting from the lowest interfacial impedance and moderate bulk resistance among the three electrolytes, the cell containing the LHCE delivered a capacity of 220 mAh g^{-1} at 4.0 C, which was over four times higher than that of a routine electrolyte and HCE [Figure 7D][89].

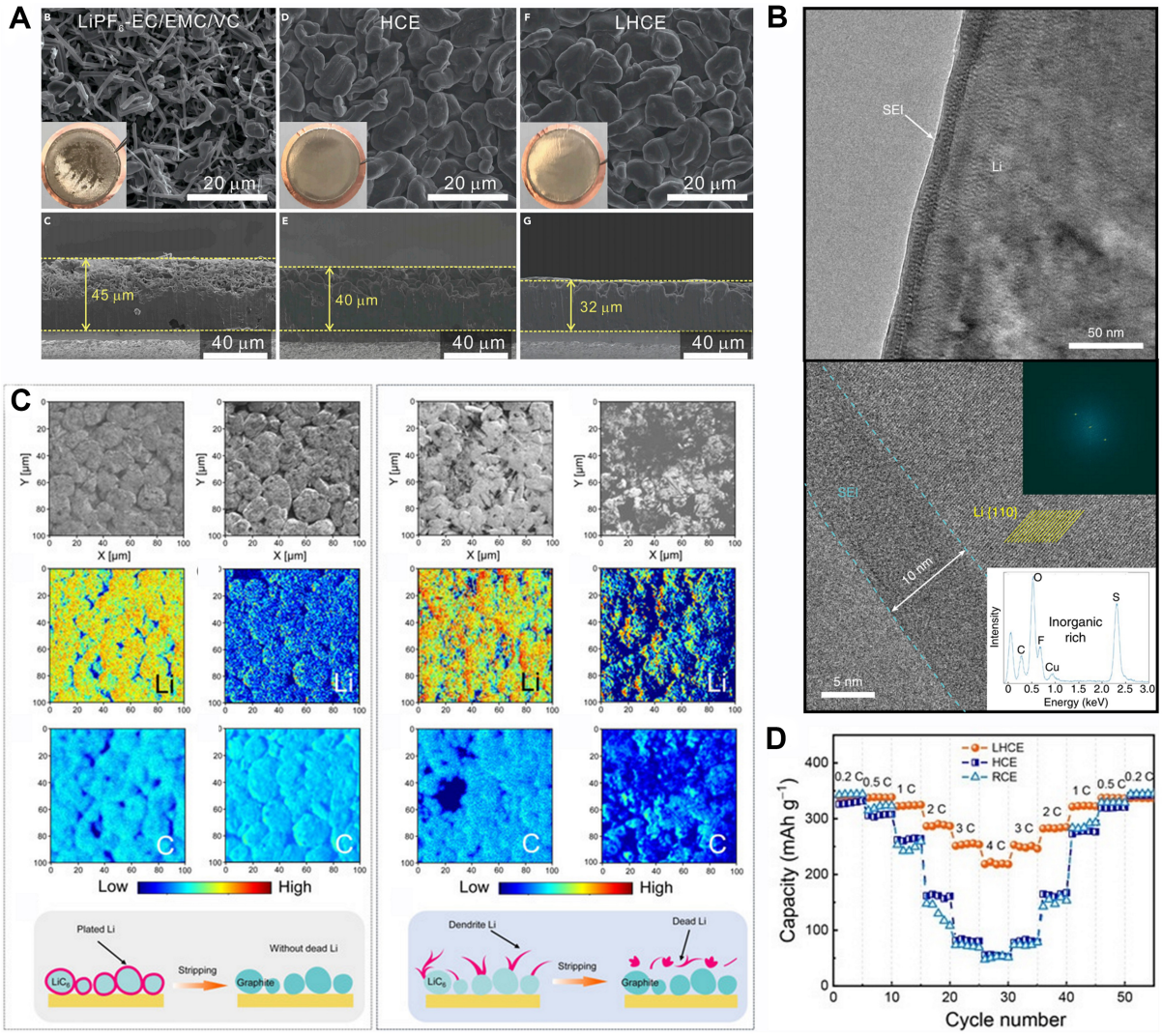

Figure 7. Interfacial properties and electrochemical performance in LHCEs. (A) Top-view and cross-sectional scanning electron microscope (SEM) images of deposited Li in various electrolytes. Reproduced with permission[121] (copyright 2019, Elsevier). (B) Cryo-electron microscopy images of SEI formed in LHCE at different scales. Insets correspond to the reduced fast Fourier transform and energy dispersive spectroscopy of SEI. Adapted with permission[122] [copyright 2019, the author(s)]. (C) Li and C elemental mapping of time-of-flight secondary ion mass spectrometry during cycling in LHCE (left) and conventional concentration electrolyte (right). Reproduced with permission[123] (copyright 2021, Wiley VCH GmbH). (D) Rate capability of graphite||Li cells using different electrolytes. Reproduced with permission[89] (copyright 2020, Wiley VCH GmbH). SEI: Solid electrolyte interphase; LHCE: localized highly concentrated electrolyte.

The general recognition of a diluent is that it breaks the three-dimensional solution structure of a HCE and separates large ion clusters, but it is unclear whether it affects the Li^+ solvation structure and the formation of the SEI. In some LHCEs, the diluent weakens the coordination of anions with Li^+[98,124], while in other LHCEs, this situation is reversed[93]. The root of these contradictory conclusions lies in the binding strength distinction of diluents and base solvents toward Li^+. The polarity of the diluent needs to be properly selected, as poor miscibility with the original electrolyte can be expected when the polarity is too low, while the Li^+ solvation structure of the HCE will be destroyed when the polarity is too high.

Cao *et al.*[125] specifically investigated the solvation structure of various fluorinated co-solvents in a LHCE via ab initio molecular dynamics simulations. As shown in Figure 8A, the radial distribution of the components in the LHCE indicates that some diluents can enter the second solvation shell to participate in the coordination with Li^+, thereby interfering with the interaction between the anions and Li^+ in the HCE, as well as the anion-derived SEI chemistry. In contrast, Piao *et al.*[99] found that the interaction between anions and Li^+ was enhanced when the TTE counter solvent was added to the LiFSI/DMC concentrated electrolyte (T3). Figure 8B demonstrates the increased proportion of highly FSI^--coordinated Li^+ (AGG-III, FSI^- complexing with over 3 Li^+) based on molecular dynamics simulations, which induces a LiF-rich SEI compared to the HCE (D7). Recently, Ding *et al.*[126] revealed the underlying mechanism of co-solvent effects in LHCEs. Specifically, the low-polarity diluent provides a low-dielectric environment, where more anions associate with Li^+ to form AGG structures. Under the electrostatic attraction of the negatively charged Li anode[127], the positively charged AGG aggregates can approach the electrode surface and are preferentially reduced to govern the SEI chemistry [Figure 8C][128].

Moreover, a solvent diagram was drawn to correlate the relative binding energy and dielectric constant, providing a guiding criterion for the choice of co-solvents [Figure 8D][126]. The choice of base solvents also has a crucial influence on the formation of the SEI. Li *et al.*[129] systematically compared the discrepancies between ether- and ester-based LHCE systems in high-voltage Li metal batteries. DFT calculations revealed that the Li^+-DME complex had a higher LUMO energy level than that of Li^+-DMC, i.e., the Li^+-DME complex was more compatible with Li electrodes due to its higher reductive stability. Therefore, the anionic decomposition on the surface of the Li electrodes was dominant in the ether-based LHCE, as also proved by the existence of the complete anion decomposed products found in the SEI according to the XPS results. Through the screening of low-polarity base solvents with higher LUMO energy levels, Xu *et al.*[130] designed a LHCE that could achieve a high CE under demanding conditions (99.7% at 1.0 mA cm^{-2}, 3.0 mAh cm^{-2}). This stemmed from the optimized interfacial structure and reduced SEI generation/reconstruction.

WSEs

In addition to tuning the salt/solvent ratio by the increasing salt concentration, reducing the intrinsic solvating power of solvents is another method used to force anions into the inner solvation shell of Li^+. From this perspective, Yao *et al.*[80] proposed the concept of a WSE, where only a solvent with weak solvation power was adopted. On this basis, abundant CIP and AGG structures in HCEs and LHCEs were inherited at a considerably low salt concentration (1.0 M), thereby circumventing the cost and intricate interaction among multicomponents. Figure 9A illustrates the change in binding energy between Li^+ with solvents and anions in different solvents acquired from DFT calculations. The relative binding energy (defined as the difference between the binding energy of Li^+-solvent and Li^+-anion, E_S-E_A) is the largest in the non-polar solvent, 1,4-dioxane, which manifests that anions prevail in the competitive coordination with Li^+. Consequently, it can be preferentially decomposed to form an anion-induced SEI.

As shown in Figure 9B, such interfacial chemistry results in a lower activation energy of Li^+ desolvation and transport through the SEI according to the results of temperature-dependent impedance tests using a three-electrode setup, which renders rapid interfacial kinetics in favor of the fast-charging performance. Lee and Pham[101] introduced another ether-based solvent of 1,2-diethoxyethane (DEE) with a low permittivity as a single solvent. Raman spectroscopy illustrated that the low solvation capability of DEE explicitly increased the ratio of anion ligands, including CIP and AGG structures, at normal concentrations [Figure 9C][101,131], contributing to LiF-rich robust passivation layers on both electrodes. In earlier work, Yu *et al.*[117] synthesized a fluorinated 1,4-dimethoxylbutane solvent and identified its low solvation ability with Li^+, incurring a high anion/solvent ratio in the solvation sheath. Such a solvation structure induced the anion-derived SEI, presenting thin, amorphous, inorganic-rich and homogeneous characteristics [Figure 9D][117].

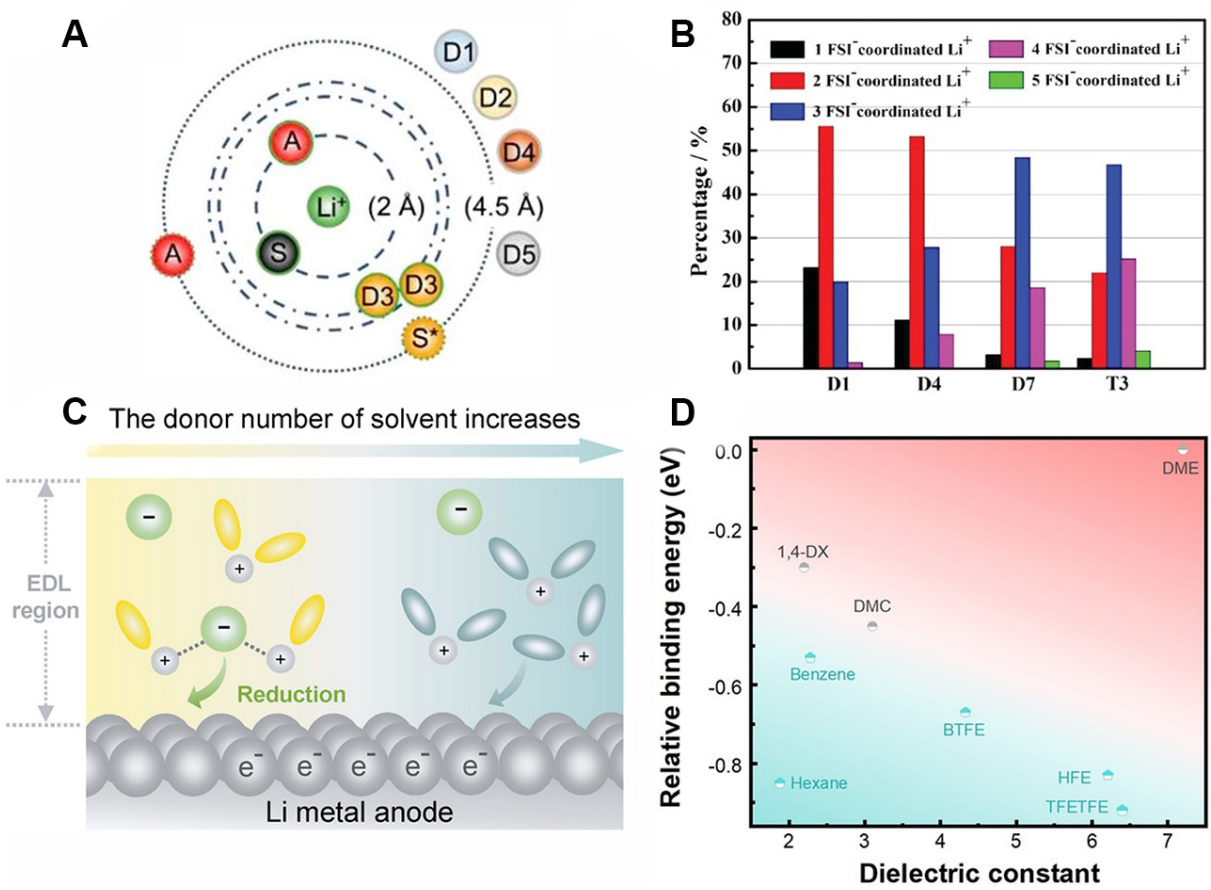

Figure 8. Mechanistic understanding of LHCEs. (A) Radial distribution of solvents, anions and different diluents. Adapted with permission[125] [copyright 2021, the author(s)]. (B) Percentage of Li^+ coordinated with different numbers of FSI^- in dilute electrolytes (D1 and D4), HCE (D7) and LHCE (T3) based on molecular dynamics simulations. Reproduced with permission[99] (copyright 2020, WILEY VCH Verlag GmbH & Co. KGaA, Weinheim). (C) Schematic of anion-cation coordination for anion-derived SEI via regulation of the electric double layer. Reproduced with permission[128] (copyright 2020, WILEY VCH GmbH). (D) Solvent diagram dependent on dielectric constant and relative binding energy (compared to DME). The solvents in the cyan region can enhance the coordination between Li^+ and anions, which facilitates the generation of the anion-derived SEI. Reproduced with permission[126] (copyright 2021, WILEY VCH GmbH). SEI: Solid electrolyte interphase; LHCE: localized highly concentrated electrolyte; HCE: highly concentrated electrolyte; FSI^-: bis(fluorosulfonyl)imide.

Under the protection of the superior SEI, the Li metal anode achieved highly-efficient cycling with a CE of 99.52%. Industrial anode-free pouch cells achieved a ~325 Wh kg^{-1} single-cell energy density and 80% capacity retention after 100 cycles.

In addition to the above single-solvent WSEs, some electrolyte systems, where weakly coordinated solvents are utilized to partially substitute for polar ones, have also been reported. In order to revive the PC electrolyte system with high-voltage cathode compatibility and a wide liquid range, Liu *et al.*[102] introduced weak-polarity diethyl carbonate (DEC) into a $LiPF_6$/PC electrolyte to decrease the coordination number of solvents with Li^+. As exhibited in Figure 10A, a more negative charge accumulated on the PC molecule (Li^+/PC-DEC = 1:5, molar ratio), which increased the LUMO energy level of PC and enhanced the reduction endurance. In another work, a low-density monoether, methyl propyl ether (MPE), with appropriate polarity and stability against Li was added to the electrolyte[100]. Under the function of weakly coordinated MPE, $TFSI^-$ was subjected to intensive coordination with Li^+, which was responsible for the prominently enhanced LiF peak in the SEI compared with the control sample [Figure 10B][100]. Recently, Kim *et al.*[132]

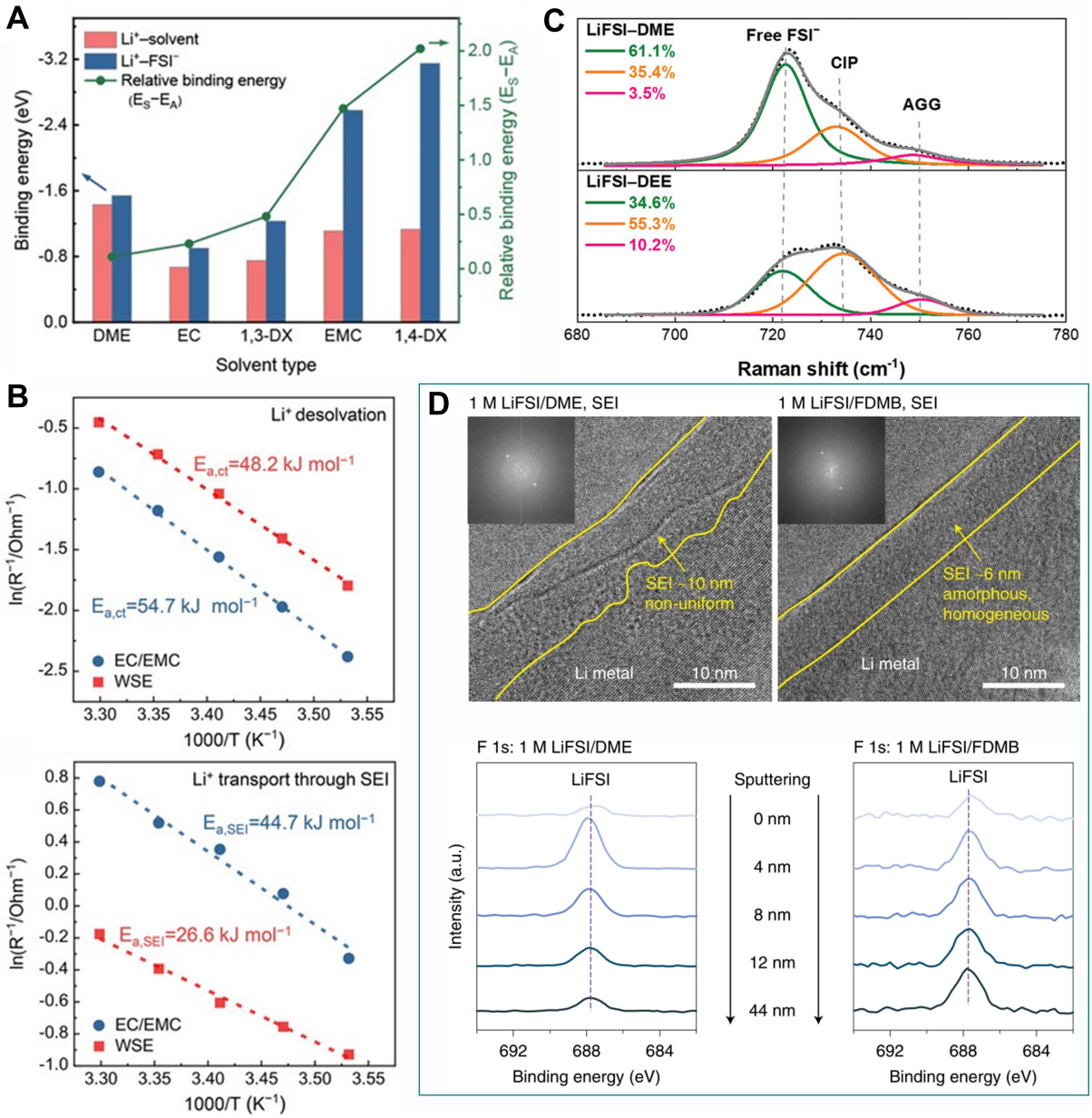

Figure 9. Characteristics and derived SEI of WSEs. (A) Binding energy of Li^+ with solvents and anions based on DFT calculations. (B) Activation energy for Li^+ desolvation and transport across the SEI in different electrolytes obtained by temperature-dependent three-electrode electrochemical impedance spectroscopy. Reproduced with permission[80] (copyright 2019, Wiley VCH GmbH). (C) Raman spectra and decoupled three-type stretching vibrations environments of FSI^- in different electrolytes. Reproduced with permission[101] (copyright 2021, Wiley VCH GmbH). (D) Cryo-electron microscopy images and F 1s XPS depth profiles of Li anode surface. Adapted with permission[117] [copyright 2020, the author(s)]. SEI: Solid electrolyte interphase; WSE: weakly solvating electrolyte; DFT: density functional theory ; FSI^-: bis(fluorosulfonyl)imide; XPS: X-ray photoelectron spectroscopy.

established the relationship between solvation energy and Li electrode cyclability, which lies in the strong correlation among Li^+ solvation structure, interfacial chemistry and the reversibility of Li cycling, as depicted in Figure 10C. In the weak binding solvent, more anions participate in the solvation structure to dominate the SEI chemistry. As-formed anion-derived SEIs composed of abundant inorganics are often conducive to the efficient utilization of Li[133].

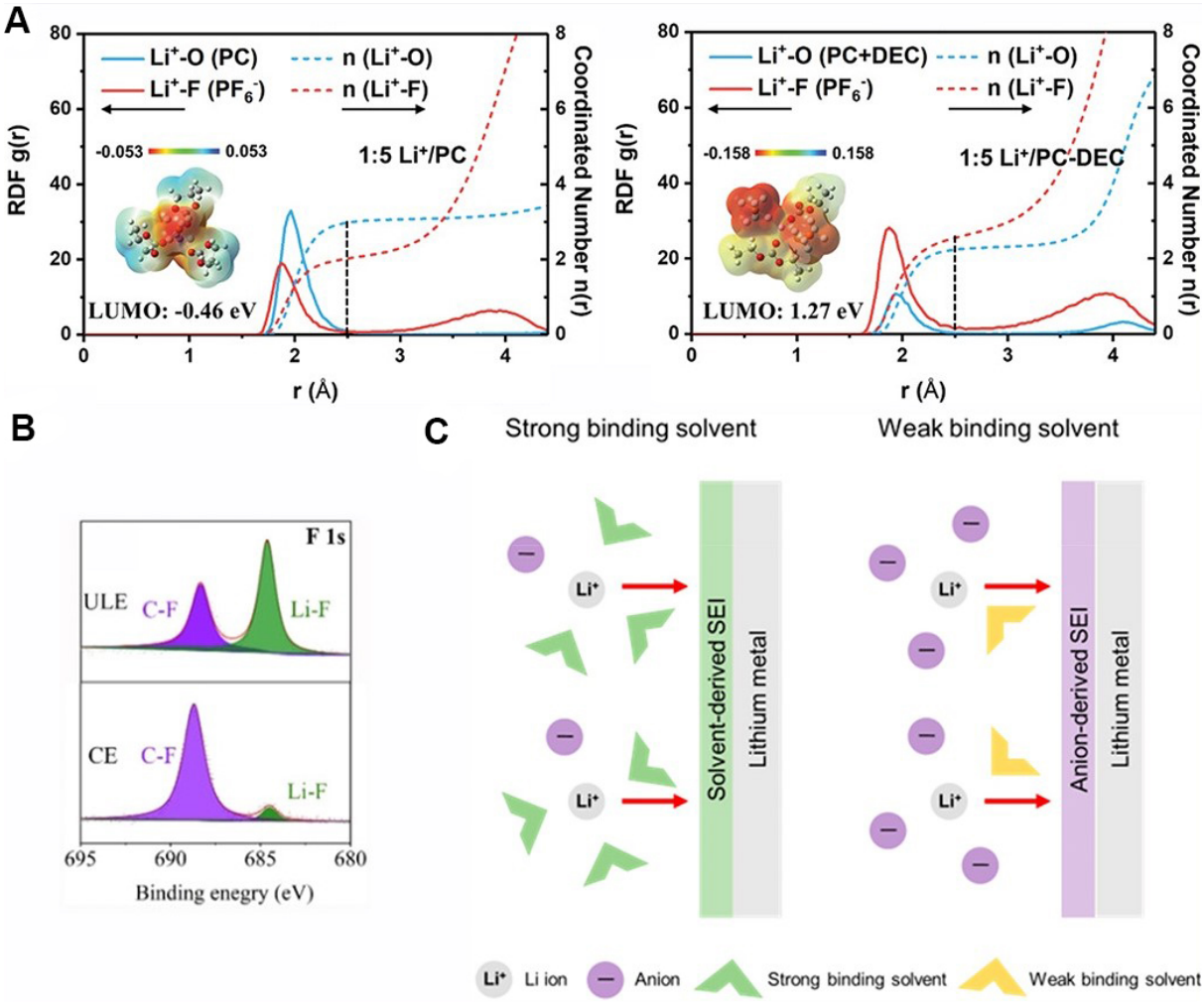

Figure 10. Solvation characteristics and induced interfacial chemistry of weakly solvating electrolytes (WSEs). (A) Radial distribution function (RDF) and coordination number of different electrolytes. Insets show the electrostatic potential mapping of typical solvation structures. Reproduced with permission[102] (copyright 2021, Wiley VCH GmbH). (B) F 1s XPS spectra of Li anode surface in WSE (ULE) and conventional electrolyte (CE). Reproduced with permission[100] (copyright 2021, Wiley VCH GmbH). (C) Schematic of correlation among the binding power of solvents, solvation structures and the formation of SEI. Reproduced with permission[132] (copyright 2021, American Chemical Society).

CONCLUSIONS AND PROSPECTS

The development of fast-charging and stable batteries is strongly reliant on the design of advanced electrolytes. Current commercial ester electrolytes no longer meet the requirements for high-rate, long-life and safe batteries, let alone for applications under demanding conditions, such as high- and low-temperature scenarios. By regulating the solvation structure, the properties of the corresponding electrolyte bulk and electrode/electrolyte interfaces are altered, which is expected to remove the constraints from traditional electrolyte systems.

HCEs generate a solvated structure with deficient solvents by virtue of a higher salt concentration, which promotes the coordination of anions and improves the reductive and oxidative stability of the system. The as-formed anion-derived SEI has an indispensable role in tolerating parasitic reactions and optimizing interfacial Li^+ transport. Furthermore, HCEs bestow an extended voltage window and ameliorative safety upon Li batteries, although they compromise the electrolyte viscosity and bulk ionic conductivity. In this

regard, the introduction of inert diluents separates the electrochemical properties of HCEs from their physicochemical characteristics, thereby solving the bulk issue specifically. LHCEs not only improve the wetting and bulk transport but also further facilitate anions to participate in the solvation of Li^+. Consequently, the elaborate bulk properties and anion-dominated SEI with abundant inorganic components significantly expand the operating temperature range, fast-charging capability and stability of Li batteries. Another method for anion-derived SEI involves adjusting the intrinsic solvation power of solvents. The weakly coordinated solvents adopted in the WSEs favor more anions into the solvation sheath, which facilitates their decomposition, even at low salt concentrations, to form an anion-derived SEI with fast interfacial kinetics.

The bulk properties and cost of HCEs limit their practical application. In addition, WSEs require a careful screening for suitable solvents to balance the solvation ability and the dissolution ability of Li salts. In comparison, LHCEs can be considered as "all-rounders" and have excellent potential as next-generation cutting-edge electrolyte systems, considering their superior performance and high design flexibility. Related spectroscopy, nuclear magnetism, cryo-electron microscopy and theoretical calculations have provided a wealth of information regarding the solvation structure, thermodynamic characteristics and interfacial composition and structure of electrodes in these emerging electrolytes. It is generally accepted that the solvation structure predominates in the formation and evolution of electrode interfaces. However, there are still gaps in the correlation between interfacial chemistry and electrode electrochemical performance in guiding rational design, and advanced characterization technology, fresh viewpoints and novel theories are strongly needed to bridge them in order to pursue future research breakthroughs in the battery community.

It is noteworthy that SEIs will undergo rupture and reconstruction during dynamic evolution, especially on host-free Li electrodes. Consequently, the lithium salt is gradually consumed to repair the anion-derived SEI and the accumulated SEI also increases battery polarization. A rigid SEI that is rich in inorganics may poorly withstand the mechanical deformation of the electrode. The combination of organic and inorganic constituents in an optimized spatial structure is expected to achieve the design of interfaces with high toughness, stability and ionic conductivity.

DECLARATIONS

Authors' contributions

Proposed the topic of this review: Huang JQ
Prepared the manuscript: Xiao Y, Xu R
Collectively discussed and revised the manuscript: Xiao Y, Xu R, Xu L, Ding JF, Huang JQ

Availability of data and materials

Not applicable.

Financial support and sponsorship

This work was supported by the Beijing Natural Science Foundation (JQ20004) and Scientific and Technological Key Project of Shanxi Province (20191102003).

Conflicts of interest

Not applicable.

Ethical approval and consent to participate

Not applicable.

Consent for publication

Not applicable.

REFERENCES

1. Bui M, Adjiman CS, Bardow A, et al. Carbon capture and storage (CCS): the way forward. *Energy Environ Sci* 2018;11:1062-176. DOI
2. Sterba J, Krzemień A, Riesgo Fernández P, Escanciano García-miranda C, Fidalgo Valverde G. Lithium mining: accelerating the transition to sustainable energy. *Resources Policy* 2019;62:416-26. DOI
3. Cheng X, Liu H, Yuan H, et al. A perspective on sustainable energy materials for lithium batteries. *SusMat* 2021;1:38-50. DOI
4. Watari T, Nansai K, Nakajima K, McLellan BC, Dominish E, Giurco D. Integrating circular economy strategies with low-carbon scenarios: lithium use in electric vehicles. *Environ Sci Technol* 2019;53:11657-65. DOI PubMed
5. Sadhukhan J, Christensen M. An in-depth life cycle assessment (LCA) of lithium-ion battery for climate impact mitigation strategies. *Energies* 2021;14:5555. DOI
6. Liu J, Yuan H, Tao X, et al. Recent progress on biomass-derived ecomaterials toward advanced rechargeable lithium batteries. *EcoMat* 2020:2. DOI
7. Shen X, Zhang X, Ding F, et al. Advanced electrode materials in lithium batteries: retrospect and prospect. *Energy Mater Adv* 2021;2021:1-15. DOI
8. Li M, Lu J, Chen Z, Amine K. 30 years of lithium-ion batteries. *Adv Mater* 2018;30:e1800561. DOI PubMed
9. Kong L, Tang C, Peng H, Huang J, Zhang Q. Advanced energy materials for flexible batteries in energy storage: a review. *SmartMat* 2020;1:1-35. DOI
10. Lin D, Liu Y, Cui Y. Reviving the lithium metal anode for high-energy batteries. *Nat Nanotechnol* 2017;12:194-206. DOI PubMed
11. Lu Y, Rong X, Hu Y, Chen L, Li H. Research and development of advanced battery materials in China. *Energy Storage Mater* 2019;23:144-53. DOI
12. Sun C, Dong J, Lu X, Li Y, Lai C. Sol electrolyte: pathway to long-term stable lithium metal anode. *Adv Funct Mater* 2021;31:2100594. DOI
13. Zhang Q, Zhang X, Yuan H, Huang J. Thermally stable and nonflammable electrolytes for lithium metal batteries: progress and perspectives. *Small Sci* 2021;1:2100058. DOI
14. Cheng XB, Zhang R, Zhao CZ, Zhang Q. Toward safe lithium metal anode in rechargeable batteries: a review. *Chem Rev* 2017;117:10403-73. DOI PubMed
15. Ding J, Xu R, Yan C, Li B, Yuan H, Huang J. A review on the failure and regulation of solid electrolyte interphase in lithium batteries. *J Energy Chem* 2021;59:306-19. DOI
16. Yan C, Yuan H, Park HS, Huang J. Perspective on the critical role of interface for advanced batteries. *J Energy Chem* 2020;47:217-20. DOI
17. Takenaka N, Bouibes A, Yamada Y, Nagaoka M, Yamada A. Frontiers in theoretical analysis of solid electrolyte interphase formation mechanism. *Adv Mater* 2021;33:e2100574. DOI PubMed
18. Liu W, Liu P, Mitlin D. Review of emerging concepts in SEI analysis and artificial SEI membranes for lithium, sodium, and potassium metal battery anodes. *Adv Energy Mater* 2020;10:2002297. DOI
19. Yan C, Xu R, Xiao Y, et al. Toward critical electrode/electrolyte interfaces in rechargeable batteries. *Adv Funct Mater* 2020;30:1909887. DOI
20. Meng X, Xu Y, Cao H, et al. Internal failure of anode materials for lithium batteries - a critical review. *Green Energy Environ* 2020;5:22-36. DOI
21. Goodenough JB, Kim Y. Challenges for rechargeable Li batteries. *Chem Mater* 2010;22:587-603. DOI PubMed
22. Yan C, Li HR, Chen X, et al. Regulating the inner helmholtz plane for stable solid electrolyte interphase on lithium metal anodes. *J Am Chem Soc* 2019;141:9422-9. DOI PubMed
23. Chen X, Li HR, Shen X, Zhang Q. The origin of the reduced reductive stability of ion-solvent complexes on alkali and alkaline earth metal anodes. *Angew Chem Int Ed Engl* 2018;57:16643-7. DOI PubMed
24. Song W, Scholtis ES, Sherrell PC, et al. Electronic structure influences on the formation of the solid electrolyte interphase. *Energy Environ Sci* 2020;13:4977-89. DOI
25. Groß A, Sakong S. Modelling the electric double layer at electrode/electrolyte interfaces. *Curr Opin Electrochem* 2019;14:1-6. DOI
26. Camacho-forero LE, Balbuena PB. Effects of charged interfaces on electrolyte decomposition at the lithium metal anode. *J Power Sources* 2020;472:228449. DOI
27. Shi S, Lu P, Liu Z, et al. Direct calculation of Li-ion transport in the solid electrolyte interphase. *J Am Chem Soc* 2012;134:15476-87. DOI PubMed
28. Peled E, Golodnitsky D, Ardel G. Advanced model for solid electrolyte interphase electrodes in liquid and polymer electrolytes. *J Electrochem Soc* 1997;144:L208-10. DOI
29. Zhang X, Cheng X, Zhang Q. Advances in interfaces between Li metal anode and electrolyte. *Adv Mater Interfaces* 2018;5:1701097.

DOI

30. Li S, Jiang M, Xie Y, Xu H, Jia J, Li J. Developing high-performance lithium metal anode in liquid electrolytes: challenges and progress. *Adv Mater* 2018;30:e1706375. DOI PubMed
31. Zhang X, Cheng X, Chen X, Yan C, Zhang Q. Fluoroethylene carbonate additives to render uniform Li deposits in lithium metal batteries. *Adv Funct Mater* 2017;27:1605989. DOI
32. Gao Y, Rojas T, Wang K, et al. Low-temperature and high-rate-charging lithium metal batteries enabled by an electrochemically active monolayer-regulated interface. *Nat Energy* 2020;5:534-42. DOI
33. Xiao Y, Xu R, Yan C, Liang Y, Ding J, Huang J. Waterproof lithium metal anode enabled by cross-linking encapsulation. *Sci Bull* 2020;65:909-16. DOI
34. Dai H, Gu X, Dong J, Wang C, Lai C, Sun S. Stabilizing lithium metal anode by octaphenyl polyoxyethylene-lithium complexation. *Nat Commun* 2020;11:643. DOI PubMed PMC
35. Xu R, Zhang X, Cheng X, et al. Artificial soft-rigid protective layer for dendrite-free lithium metal anode. *Adv Funct Mater* 2018;28:1705838. DOI
36. Liu K, Pei A, Lee HR, et al. Lithium metal anodes with an adaptive "solid-liquid" interfacial protective layer. *J Am Chem Soc* 2017;139:4815-20. DOI PubMed
37. Yan C, Cheng XB, Tian Y, et al. Dual-Layered film protected lithium metal anode to enable dendrite-free lithium deposition. *Adv Mater* 2018;30:e1707629. DOI PubMed
38. Zheng G, Lee SW, Liang Z, et al. Interconnected hollow carbon nanospheres for stable lithium metal anodes. *Nat Nanotechnol* 2014;9:618-23. DOI PubMed
39. Xu R, Xiao Y, Zhang R, et al. Dual-phase single-ion pathway interfaces for robust lithium metal in working batteries. *Adv Mater* 2019;31:e1808392. DOI PubMed
40. Yan C, Cheng XB, Yao YX, et al. An armored mixed conductor interphase on a dendrite-free lithium-metal anode. *Adv Mater* 2018;30:e1804461. DOI PubMed
41. Xu R, Cheng X, Yan C, et al. Artificial interphases for highly stable lithium metal anode. *Matter* 2019;1:317-44. DOI
42. Cai W, Yan C, Yao Y, et al. Rapid lithium diffusion in order@disorder pathways for fast-charging graphite anodes. *Small Struct* 2020;1:2000010. DOI
43. Cai W, Yao YX, Zhu GL, et al. A review on energy chemistry of fast-charging anodes. *Chem Soc Rev* 2020;49:3806-33. DOI PubMed
44. Logan E, Dahn J. Electrolyte design for fast-charging li-ion batteries. *Trends Chem* 2020;2:354-66. DOI
45. Yamada Y, Wang J, Ko S, Watanabe E, Yamada A. Advances and issues in developing salt-concentrated battery electrolytes. *Nat Energy* 2019;4:269-80. DOI
46. Yan C, Jiang LL, Yao YX, Lu Y, Huang JQ, Zhang Q. Nucleation and growth mechanism of anion-derived solid electrolyte interphase in rechargeable batteries. *Angew Chem Int Ed Engl* 2021;60:8521-5. DOI PubMed
47. Scharifker B, Hills G. Theoretical and experimental studies of multiple nucleation. *Electrochimica Acta* 1983;28:879-89. DOI
48. Scharifker B, Rugeles R, Mozota J. Electrocrystallization of copper sulphide (CU2S) on copper. *Electrochimica Acta* 1984;29:261-6. DOI
49. Bewick A, Fleischmann M, Thirsk HR. Kinetics of the electrocrystallization of thin films of calomel. *Trans Faraday Soc* 1962;58:2200. DOI
50. Li Z, Zhou Y, Wang Y, Lu Y. Solvent-mediated Li_2S electrodeposition: a critical manipulator in lithium-sulfur batteries. *Adv Energy Mater* 2019;9:1802207. DOI
51. Wu H, Jia H, Wang C, Zhang J, Xu W. Recent progress in understanding solid electrolyte interphase on lithium metal anodes. *Adv Energy Mater* 2021;11:2003092. DOI
52. Suo L, Xue W, Gobet M, et al. Fluorine-donating electrolytes enable highly reversible 5-V-class Li metal batteries. *Proc Natl Acad Sci U S A* 2018;115:1156-61. DOI PubMed PMC
53. Xu R, Yan C, Xiao Y, Zhao M, Yuan H, Huang J. The reduction of interfacial transfer barrier of Li ions enabled by inorganics-rich solid-electrolyte interphase. *Energy Storage Mater* 2020;28:401-6. DOI
54. Chen X, Zhang Q. Atomic Insights into the fundamental interactions in lithium battery electrolytes. *Acc Chem Res* 2020;53:1992-2002. DOI PubMed
55. Peled E, Menkin S. Review-SEI: past, present and future. *J Electrochem Soc* 2017;164:A1703-19. DOI
56. Zhao J, Liao L, Shi F, et al. Surface fluorination of reactive battery anode materials for enhanced stability. *J Am Chem Soc* 2017;139:11550-8. DOI PubMed
57. Chen YC, Ouyang CY, Song LJ, Sun ZL. Electrical and lithium ion dynamics in three main components of solid electrolyte interphase from density functional theory study. *J Phys Chem C* 2011;115:7044-9. DOI
58. Lin D, Liu Y, Chen W, et al. Conformal lithium fluoride protection layer on three-dimensional lithium by nonhazardous gaseous reagent Freon. *Nano Lett* 2017;17:3731-7. DOI PubMed
59. Monroe C, Newman J. The impact of elastic deformation on deposition kinetics at lithium/polymer interfaces. *J Electrochem Soc* 2005;152:A396. DOI
60. Wu M, Wen Z, Liu Y, Wang X, Huang L. Electrochemical behaviors of a Li3N modified Li metal electrode in secondary lithium batteries. *J Power Sources* 2011;196:8091-7. DOI
61. Zhang Y, Wang W, Tang H, et al. An ex-situ nitridation route to synthesize Li 3 N-modified Li anodes for lithium secondary batteries. *J Power Sources* 2015;277:304-11. DOI

62. Billone M, Liu Y, Poeppel R, Routbort J, Goretta K, Kupperman D. Elastic and creep properties of Li_2O. *J Nucl Mater* 1986;141-143:282-8. DOI
63. Huang W, Attia PM, Wang H, et al. Evolution of the solid-electrolyte interphase on carbonaceous anodes visualized by atomic-resolution cryogenic electron microscopy. *Nano Lett* 2019;19:5140-8. DOI PubMed
64. Cheng X, Yan C, Chen X, et al. Implantable solid electrolyte interphase in lithium-metal batteries. *Chem* 2017;2:258-70. DOI
65. Shen X, Zhang R, Chen X, Cheng X, Li X, Zhang Q. The failure of solid electrolyte interphase on li metal anode: structural uniformity or mechanical strength? *Adv Energy Mater* 2020;10:1903645. DOI
66. Ramasubramanian A, Yurkiv V, Foroozan T, Ragone M, Shahbazian-yassar R, Mashayek F. Lithium diffusion mechanism through solid-electrolyte interphase in rechargeable lithium batteries. *J Phys Chem C* 2019;123:10237-45. DOI
67. Ahmad Z, Venturi V, Hafiz H, Viswanathan V. Interfaces in solid electrolyte interphase: implications for lithium-ion batteries. *J Phys Chem C* 2021;125:11301-9. DOI
68. Chen XR, Yao YX, Yan C, Zhang R, Cheng XB, Zhang Q. A diffusion-reaction competition mechanism to tailor lithium deposition for lithium-metal batteries. *Angew Chem Int Ed Engl* 2020;59:7743-7. DOI PubMed
69. Cui C, Yang C, Eidson N, et al. A highly reversible, dendrite-free lithium metal anode enabled by a lithium-fluoride-enriched interphase. *Adv Mater* 2020;32:e1906427. DOI PubMed
70. Zheng J, Ju Z, Zhang B, et al. Lithium ion diffusion mechanism on the inorganic components of the solid–electrolyte interphase. *J Mater Chem A* 2021;9:10251-9. DOI
71. Fan X, Ji X, Han F, et al. Fluorinated solid electrolyte interphase enables highly reversible solid-state Li metal battery. *Sci Adv* 2018;4:eaau9245. DOI PubMed PMC
72. Li W, Wu G, Araújo CM, et al. Li+ ion conductivity and diffusion mechanism in α-Li_3N and β-Li_3N. *Energy Environ Sci* 2010;3:1524. DOI
73. Zhu J, Li P, Chen X, et al. Rational design of graphitic-inorganic Bi-layer artificial SEI for stable lithium metal anode. *Energy Storage Mater* 2019;16:426-33. DOI
74. Moradabadi A, Kaghazchi P. Thermodynamics and kinetics of defects in Li_2S. *Appl Phys Lett* 2016;108:213906. DOI
75. Borodin O, Zhuang GV, Ross PN, Xu K. Molecular dynamics simulations and experimental study of lithium ion transport in dilithium ethylene dicarbonate. *J Phys Chem C* 2013;117:7433-44. DOI
76. Chen X, Zhang X, Li H, Zhang Q. Cation-solvent, cation-anion, and solvent-solvent interactions with electrolyte solvation in lithium batteries. *Batteries & Supercaps* 2019;2:128-31. DOI
77. Yamada Y, Yamada A. Review - superconcentrated electrolytes for lithium batteries. *J Electrochem Soc* 2015;162:A2406-23. DOI
78. Zheng J, Lochala JA, Kwok A, Deng ZD, Xiao J. Research progress towards understanding the unique interfaces between concentrated electrolytes and electrodes for energy storage applications. *Adv Sci (Weinh)* 2017;4:1700032. DOI PubMed PMC
79. Seo DM, Borodin O, Han S, Ly Q, Boyle PD, Henderson WA. Electrolyte solvation and ionic association. *J Electrochem Soc* 2012;159:A553-65. DOI
80. Yao YX, Chen X, Yan C, et al. Regulating interfacial chemistry in lithium-ion batteries by a weakly solvating electrolyte*. *Angew Chem Int Ed Engl* 2021;60:4090-7. DOI PubMed
81. Suo L, Hu YS, Li H, Armand M, Chen L. A new class of Solvent-in-Salt electrolyte for high-energy rechargeable metallic lithium batteries. *Nat Commun* 2013;4:1481. DOI PubMed
82. Wang J, Yamada Y, Sodeyama K, Chiang CH, Tateyama Y, Yamada A. Superconcentrated electrolytes for a high-voltage lithium-ion battery. *Nat Commun* 2016;7:12032. DOI PubMed PMC
83. Yamada Y, Chiang CH, Sodeyama K, Wang J, Tateyama Y, Yamada A. Corrosion prevention mechanism of aluminum metal in superconcentrated electrolytes. *ChemElectroChem* 2015;2:1687-94. DOI
84. Li M, Wang C, Chen Z, Xu K, Lu J. New concepts in electrolytes. *Chem Rev* 2020;120:6783-819. DOI PubMed
85. Qian J, Henderson WA, Xu W, et al. High rate and stable cycling of lithium metal anode. *Nat Commun* 2015;6:6362. DOI PubMed PMC
86. Fan X, Chen L, Ji X, et al. Highly fluorinated interphases enable high-voltage Li-metal batteries. *Chem* 2018;4:174-85. DOI
87. Wang J, Yamada Y, Sodeyama K, et al. Fire-extinguishing organic electrolytes for safe batteries. *Nat Energy* 2018;3:22-9. DOI
88. Jiao S, Ren X, Cao R, et al. Stable cycling of high-voltage lithium metal batteries in ether electrolytes. *Nat Energy* 2018;3:739-46. DOI
89. Jiang LL, Yan C, Yao YX, Cai W, Huang JQ, Zhang Q. Inhibiting solvent Co-intercalation in a graphite anode by a localized high-concentration electrolyte in fast-charging batteries. *Angew Chem Int Ed Engl* 2021;60:3402-6. DOI PubMed
90. Yamada Y, Furukawa K, Sodeyama K, et al. Unusual stability of acetonitrile-based superconcentrated electrolytes for fast-charging lithium-ion batteries. *J Am Chem Soc* 2014;136:5039-46. DOI PubMed
91. Takenaka N, Fujie T, Bouibes A, Yamada Y, Yamada A, Nagaoka M. Microscopic formation mechanism of solid electrolyte interphase film in lithium-ion batteries with highly concentrated electrolyte. *J Phys Chem C* 2018;122:2564-71. DOI
92. Fan X, Ji X, Chen L, et al. All-temperature batteries enabled by fluorinated electrolytes with non-polar solvents. *Nat Energy* 2019;4:882-90. DOI
93. Jiang Z, Zeng Z, Liang X, et al. Fluorobenzene, a low-density, economical, and bifunctional hydrocarbon cosolvent for practical lithium metal batteries. *Adv Funct Mater* 2021;31:2005991. DOI
94. Ren X, Chen S, Lee H, et al. Localized high-concentration sulfone electrolytes for high-efficiency lithium-metal batteries. *Chem* 2018;4:1877-92. DOI
95. Yang Y, Davies DM, Yin Y, et al. High-efficiency lithium-metal anode enabled by liquefied gas electrolytes. *Joule* 2019;3:1986-

2000. DOI
96. Cao X, Zou L, Matthews BE, et al. Optimization of fluorinated orthoformate based electrolytes for practical high-voltage lithium metal batteries. *Energy Storage Mater* 2021;34:76-84. DOI
97. Cao X, Jia H, Xu W, Zhang J. Review - localized high-concentration electrolytes for lithium batteries. *J Electrochem Soc* 2021;168:010522. DOI
98. Chen S, Zheng J, Mei D, et al. High-voltage lithium-metal batteries enabled by localized high-concentration electrolytes. *Adv Mater* 2018;30:e1706102. DOI PubMed
99. Piao N, Ji X, Xu H, et al. Countersolvent electrolytes for lithium-metal batteries. *Adv Energy Mater* 2020;10:1903568. DOI
100. Liu T, Li H, Yue J, et al. Ultralight electrolyte for high-energy lithium-sulfur pouch cells. *Angew Chem Int Ed Engl* 2021;60:17547-55. DOI PubMed
101. Pham TD, Lee KK. Simultaneous stabilization of the solid/cathode electrolyte interface in lithium metal batteries by a new weakly solvating electrolyte. *Small* 2021;17:e2100133. DOI PubMed
102. Liu X, Shen X, Li H, et al. Ethylene carbonate-free propylene carbonate-based electrolytes with excellent electrochemical compatibility for Li-ion batteries through engineering electrolyte solvation structure. *Adv Energy Mater* 2021;11:2003905. DOI
103. Jeong S, Inaba M, Iriyama Y, Abe T, Ogumi Z. Electrochemical intercalation of lithium ion within graphite from propylene carbonate solutions. *Electrochem Solid-State Lett* 2003;6:A13. DOI
104. Xing L, Zheng X, Schroeder M, et al. Deciphering the ethylene carbonate-propylene carbonate mystery in Li-ion batteries. *Acc Chem Res* 2018;51:282-9. DOI PubMed
105. Yamada Y, Yamada A. Superconcentrated electrolytes to create new interfacial chemistry in non-aqueous and aqueous rechargeable batteries. *Chem Lett* 2017;46:1056-64. DOI
106. Yamada Y, Yaegashi M, Abe T, Yamada A. A superconcentrated ether electrolyte for fast-charging Li-ion batteries. *Chem Commun (Camb)* 2013;49:11194-6. DOI PubMed
107. Wang J, Zheng Q, Fang M, Ko S, Yamada Y, Yamada A. Concentrated electrolytes widen the operating temperature range of lithium-ion batteries. *Adv Sci (Weinh)* 2021;8:e2101646. DOI PubMed PMC
108. Liu T, Lin L, Bi X, et al. In situ quantification of interphasial chemistry in Li-ion battery. *Nat Nanotechnol* 2019;14:50-6. DOI PubMed
109. Yao YX, Yan C, Zhang Q. Emerging interfacial chemistry of graphite anodes in lithium-ion batteries. *Chem Commun (Camb)* 2020;56:14570-84. DOI PubMed
110. Moon H, Tatara R, Mandai T, et al. Mechanism of Li ion desolvation at the interface of graphite electrode and glyme–Li salt solvate ionic liquids. *J Phys Chem C* 2014;118:20246-56. DOI
111. Ming J, Cao Z, Wu Y, et al. New insight on the role of electrolyte additives in rechargeable lithium ion batteries. *ACS Energy Lett* 2019;4:2613-22. DOI
112. Zhang T, Paillard E. Recent advances toward high voltage, EC-free electrolytes for graphite-based Li-ion battery. *Front Chem Sci Eng* 2018;12:577-91. DOI
113. Jeong S, Seo H, Kim D, et al. Suppression of dendritic lithium formation by using concentrated electrolyte solutions. *Electrochem Commun* 2008;10:635-8. DOI
114. Alvarado J, Schroeder MA, Pollard TP, et al. Bisalt ether electrolytes: a pathway towards lithium metal batteries with Ni-rich cathodes. *Energy Environ Sci* 2019;12:780-94. DOI
115. Zhang X, Chen X, Hou L, et al. Regulating anions in the solvation sheath of lithium ions for stable lithium metal batteries. *ACS Energy Lett* 2019;4:411-6. DOI
116. Louli AJ, Eldesoky A, Weber R, et al. Diagnosing and correcting anode-free cell failure via electrolyte and morphological analysis. *Nat Energy* 2020;5:693-702. DOI
117. Yu Z, Wang H, Kong X, et al. Molecular design for electrolyte solvents enabling energy-dense and long-cycling lithium metal batteries. *Nat Energy* 2020;5:526-33. DOI
118. Chen S, Zheng J, Yu L, et al. High-efficiency lithium metal batteries with fire-retardant electrolytes. *Joule* 2018;2:1548-58. DOI
119. Dokko K, Tachikawa N, Yamauchi K, et al. Solvate ionic liquid electrolyte for Li–S batteries. *J Electrochem Soc* 2013;160:A1304-10. DOI
120. Moon H, Mandai T, Tatara R, et al. Solvent activity in electrolyte solutions controls electrochemical reactions in Li-Ion and Li-sulfur batteries. *J Phys Chem C* 2015;119:3957-70. DOI
121. Ren X, Zou L, Cao X, et al. Enabling high-voltage lithium-metal batteries under practical conditions. *Joule* 2019;3:1662-76. DOI
122. Cao X, Ren X, Zou L, et al. Monolithic solid–electrolyte interphases formed in fluorinated orthoformate-based electrolytes minimize Li depletion and pulverization. *Nat Energy* 2019;4:796-805. DOI
123. Cai W, Yan C, Yao YX, et al. The boundary of lithium plating in graphite electrode for safe lithium-ion batteries. *Angew Chem Int Ed Engl* 2021;60:13007-12. DOI PubMed
124. Amanchukwu CV, Kong X, Qin J, Cui Y, Bao Z. Nonpolar alkanes modify lithium-ion solvation for improved lithium deposition and stripping. *Adv Energy Mater* 2019;9:1902116. DOI
125. Cao X, Gao P, Ren X, et al. Effects of fluorinated solvents on electrolyte solvation structures and electrode/electrolyte interphases for lithium metal batteries. *Proc Natl Acad Sci U S A* 2021;118:e2020357118. DOI PubMed PMC
126. Ding JF, Xu R, Yao N, et al. Non-solvating and low-dielectricity cosolvent for anion-derived solid electrolyte interphases in lithium metal batteries. *Angew Chem Int Ed Engl* 2021;60:11442-7. DOI PubMed
127. Santos E, Schmickler W. The crucial role of local excess charges in dendrite growth on lithium electrodes. *Angew Chem Int Ed Engl*

2021;60:5876-81. DOI PubMed PMC

128. Xu R, Shen X, Ma XX, et al. Identifying the critical anion-cation coordination to regulate the electric double layer for an efficient lithium-metal anode interface. *Angew Chem Int Ed Engl* 2021;60:4215-20. DOI PubMed
129. Li T, Li Y, Sun Y, Qian Z, Wang R. New insights on the good compatibility of ether-based localized high-concentration electrolyte with lithium metal. *ACS Materials Lett* 2021;3:838-44. DOI
130. Xu R, Ding JF, Ma XX, Yan C, Yao YX, Huang JQ. Designing and demystifying the lithium metal interface toward highly reversible batteries. *Adv Mater* 2021:e2105962. DOI PubMed
131. Battisti D, Nazri GA, Klassen B, Aroca R. Vibrational studies of lithium perchlorate in propylene carbonate solutions. *J Phys Chem* 1993;97:5826-30. DOI
132. Kim SC, Kong X, Vilá RA, et al. Potentiometric measurement to probe solvation energy and its correlation to lithium battery cyclability. *J Am Chem Soc* 2021;143:10301-8. DOI PubMed
133. Xue W, Huang M, Li Y, et al. Ultra-high-voltage Ni-rich layered cathodes in practical Li metal batteries enabled by a sulfonamide-based electrolyte. *Nat Energy* 2021;6:495-505. DOI